ACS APPLIED MATERIALS & INTERFACES

Research Article

www.acsami.org

Bioinspired Smart Actuator Based on Graphene Oxide-Polymer Hybrid Hydrogels

Tao Wang, Jiahe Huang, Yiqing Yang, Enzhong Zhang, Weixiang Sun, and Zhen Tong*

Research Institute of Materials Science and State Key Laboratory of Luminescent Materials and Devices, South China University of Technology, Guangzhou 510640, China

Supporting Information

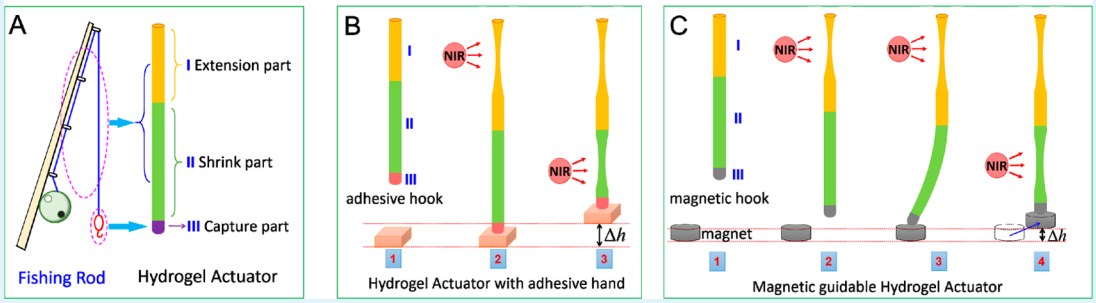

ABSTRACT: Rapid response and strong mechanical properties are desired for smart materials used in soft actuators. A bioinspired hybrid hydrogel actuator was designed and prepared by series combination of three trunks of tough polymer−clay hydrogels to accomplish the comprehensive actuation of "extension−grasp−retraction" like a fishing rod. The hydrogels with thermo-creep and thermo-shrinking features were successively irradiated by near-infrared (NIR) to execute extension and retraction, respectively. The GO in the hydrogels absorbed the NIR energy and transformed it into thermo-energy rapidly and effectively. The hydrogel with adhesion or magnetic force was adopted as the "hook" of the hybrid hydrogel actuator for grasping object. The hook of the hybrid hydrogel actuator was replaceable according to applications, even with functional materials other than hydrogels. This study provides an innovative concept to explore new soft actuators through combining response hydrogels and programming the same stimulus.

KEYWORDS: *hybrid hydrogel, response hydrogel combination, actuator, graphene oxide, bioinspired material*

INTRODUCTION

Soft actuators are soft machine capable to accomplish the actions of capture, movement, and manipulation under controlling, and the key factor of a soft actuator is the response soft materials, which are manipulated under the signal of chemical or physical stimuli.[1] Some soft actuators are designed upon the biomimetic or bioinspired principles based on the smart simulation of living organisms, animals, and mankind, and potentially utilized in biomedical and micromachine areas. Hydrogels, composed of polymer networks and large amount of water similar to the structure of natural tissues, were a strong candidate of stimuli-response materials required for the soft actuator.[2,3] However, poor mechanical strength and low extensibility restricted the conventional synthetic hydrogels to be actually applied in soft actuators.[3,4] The appearance of tough hydrogels greatly promised the application as the response material in soft actuators.[5−10] Among the stimuli-response hydrogels, the light-response hydrogel showed superior merits, such as noncontact control and simple device design.[7,11] Near-infrared (NIR) was mostly used as the driving energy and control signal for the soft actuator because of its safety and penetrating capability entering the tissues and organs.[12]

Graphene has attracted tremendous interests as a rising star material because of its unique properties,[13] which absorbs the NIR irradiation and transforms it into thermal energy quickly and efficiently.[11,14] Graphene oxide (GO) acting as physical cross-linker has been widely used in preparing stimuli-response hydrogels cooperated with other cross-linkers, such as *N*,*N*′-methylenebis(acrylamide) and clay.[6,13,15−23] In our previous work, a tough hydrogel composed of poly(*N*-isopropylacrylamide) (PNIPAAm), hectorite clay, and GO was utilized in constructing a bilayer hydrogel actuator driven by NIR irradiation,[7] where GO acted as an energy-converter. When exposed to NIR radiation, the temperature of the GO-containing hydrogel layer was always higher than that of the hydrogel layer without GO, causing the bilayer hydrogel to bend. Other soft actuators for lifting or grasping objects were also reported.[10,24−26] All of these actuators were capable to accomplish only one action because the response material used possessed single response and single action. On the other hand, a comprehensive action is desired as inspired from fishing rods

Received: April 30, 2015
Accepted: October 8, 2015
Published: October 8, 2015

DOI: 10.1021/acsami.5b08248
ACS Appl. Mater. Interfaces 2015, 7, 23423−23430

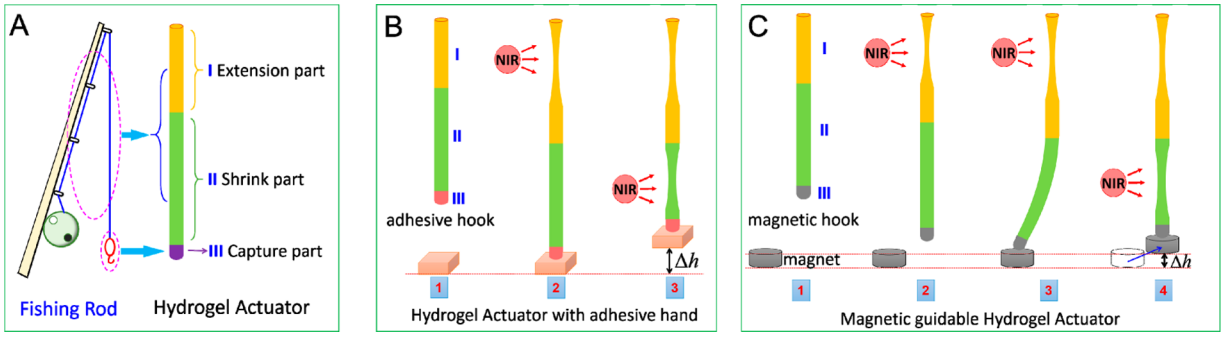

Figure 1. (A) Schema of the hybrid hydrogel actuator composed with three trunks of stimuli-response hydrogels like a fishing rod. (B) actuation of the hybrid hydrogel actuator with an adhesive hook (part III). (C) actuation of the hybrid hydrogel actuator with a magnetic hook (part III) guided by magnetic force.

Table 1. Monomer Composition of the Hydrogel Trunks Illustrated in Figure 1A

part	length (mm)	code	NIPAAm (mol/L)	DMAA (mol/L)	XLG (w/v%)	XLS (w/v%)	α-CD (w/v%)	GO (mg/mL)	Fe_3O_4 (mg/mL)
I	40	D1G2.5GO2		1.0	2.5			2.0	
II	100	N1S2GO2	1.0			2.0		2.0	
		D3G3CD8		3.0	3.0		8.0		
III	20	D3G3Fe3		3.0	3.0				3.0
		N1S2GO2CD8	1.0			2.0	8.0	2.0	

and human arms, which are achieved by combination of several movements such as approaching, grasping and lifting.

Similar to a fishing rod, we combine three trunks of hybrid hydrogels with excellent mechanical strength and extensibility in series to accomplish an "extension−grasp−retraction" comprehensive actuation (schematically illustrated in Figure 1A). NIR is chosen as the stimulus signal and driving energy, and GO is incorporated into the hydrogels to absorb the NIR energy and to transform it into thermal energy. The hydrogel trunks execute the extension (part I) and contraction (part II) actions separately driven by NIR irradiation like a fishing rod (Figure 1B). The "hook" hydrogel trunk (part III) is smartly designed with adhesion or magnetic as a hand to grasp specified objects (Figures 1B and 1C).

EXPERIMENTAL SECTION

Materials. Monomer *N*-isopropylacrylamide (NIPAAm, TCI, 1% stabilizer) was recrystallized from toluene/*n*-hexane mixture and dried in vacuum at room temperature for 48 h. Monomer *N*,*N*-dimethylacrylamide (DMAA, J&K, ≥ 98%), α-cyclodextrin (α-CD, J&K, 98%), initiator potassium peroxydisulfate ($K_2S_2O_8$, J&K, 99%), and catalyst *N*,*N*,*N*′,*N*′-tetramethylethylenediamine (TEMED, Acros, 99%) were used as received. Synthetic hectorite clay of gel-forming grade LAPONITE XLG [$Mg_{5.34}Li_{0.66}Si_8O_{20}(OH)_4Na_{0.66}$] and sol-forming grade LAPONITE XLS [92.32 wt % of $Mg_{5.34}Li_{0.66}Si_8O_{20}(OH)_4Na_{0.66}$ and 7.68 wt % of $Na_4P_2O_7$] was purchased from Rockwood, Ltd., and used after dried at 125 °C for 2 h. Preparation of Fe_3O_4 nanoparticles was described in Supporting Information. Pure water was obtained by deionization and filtration with a Millipore purification apparatus (resistivity ≥18.2 MΩ·cm) and bubbled with argon gas for more than 1 h prior to use in the gel preparation.

Preparation of GO. GO was prepared according to the modified Hummers method.[27] Two grams of graphite powder (Alfa Aesar, 325 mesh, 99.8%) and 1 g of $NaNO_3$ were added to 46 mL of cold (~0 °C) concentrated H_2SO_4 in a 250 mL flask. The mixture was stirred in an ice bath for 30 min, and 6 g of $KMnO_4$ was slowly added under vigorous stirring. The reaction was carried out for 2 h. Then, the ice bath was removed, and the reaction mixture was maintained at 35 °C for 0.5 h. Afterward, 30 mL of deionized water was gradually added into the mixture, and the reaction system was transferred to a 98 °C water bath for 15 min. Finally, 20 mL of 30% H_2O_2 was added to the mixture. For purification, the mixture was washed with 5% of HCl and deionized water several times. GO was dried at 60 °C in vacuum for 24 h.

Preparation of Hydrogel Actuators. The hybrid hydrogel actuator consisting of connected three trunks of response hydrogels was synthesized in one step. The actuator was composed of part I of PDMAA-XLG-GO gel, part II of PNIPAAm-XLS-GO gel, and part III of PDMAA-XLG-α-CD gel, PDMAA-XLG-Fe_3O_4 gel, or PNIPAAm-XLS-GO-α-CD gel. The synthesis procedure was similar to the literature method.[28] First, GO or Fe_3O_4 nanoparticle was dispersed in water for at least 2 h, and then the clay of XLG or XLS was added. The mixture was dispersed for another 2 h to produce a uniform suspension. After that, the monomer NIPAAm or DMAA was added to a specified concentration and stirred for 2 h. α-CD was then added when designed. The reaction solution was degassed before adding KPS solution (20 mg/mL) and catalyst TEMED. For the hybrid hydrogel actuator, the reaction solutions with different compositions were poured into a glass tube of 6.0 mm diameter in the sequence of parts III, II, and I for in situ polymerization. Because of the high viscosity of these reaction solutions, the depth of mutual diffusion across the interface between two gel trunks was limited, which maintained the features of each gel trunk and ensured high connection strength. The hydrogel sample used for creep measurement was polymerized in a laboratory made mold of 80 mm × 80 mm × 2 mm, which consisted of two glass substrates with a rubber spacer. The PDMAA (D1G2.5) and PNIPAAm (N1S2) hydrogel samples without GO were also synthesized for comparison. The compositions and codes of each part of the hydrogels are listed in Table 1.

NIR Driving of Hydrogel Actuators. Two halogen tungsten lamps with a filter of cutoff <600 nm were used as the NIR light source located at a distance of 50 mm from the sample on both sides. The power density delivered to the sample was about 0.5 Wcm^{-2} on each side. Parts I and II of the hydrogel actuator were irradiated successively for a desired time, and the length of the entire hybrid hydrogel actuator during irradiation was recorded.

To explore the NIR irradiation effect on the PDMAA and PNIPAAm hydrogels with and without GO, the length and temperature were measured as a function of irradiation time. Repeat actuation circle of the hybrid hydrogel actuator was tested in two procedures: One is that parts I and II were merely irradiated successively for 30 and 60 s for several times. Another is that the hydrogel was immersed in deionized water at room temperature for 15

DOI: 10.1021/acsami.5b08248
ACS Appl. Mater. Interfaces 2015, 7, 23423−23430

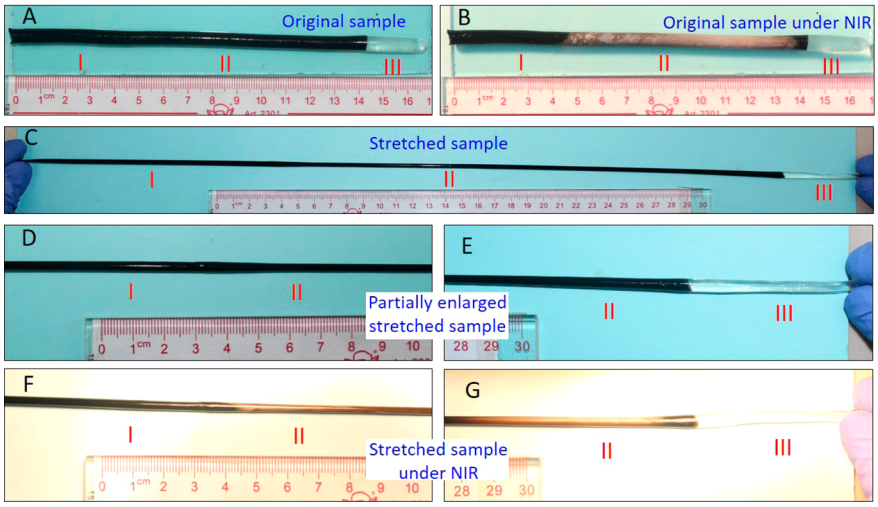

Figure 2. Photos of the actuating hydrogel (D1G2.5GO2 + N1S2GO2 + D3G3CD8). A: Original sample. B: Hydrogel sample under NIR irradiation. C: Hydrogel sample under stretch. D and E: Enlarged junction area of the stretched sample. F and G: Enlarged junction area of the stretched sample under NIR irradiation.

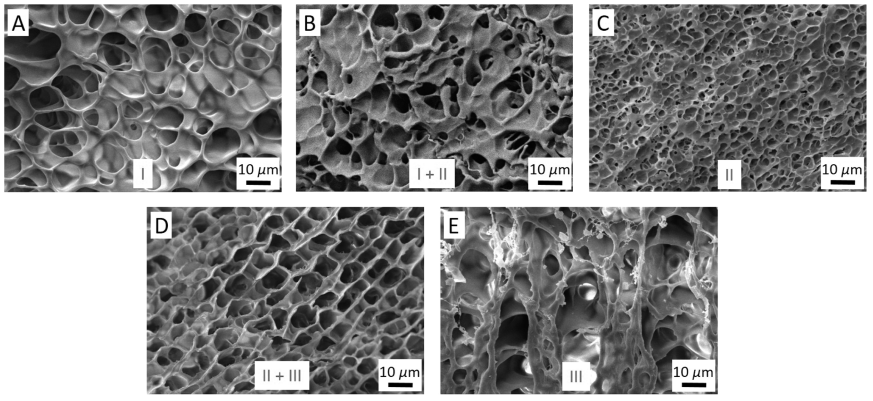

Figure 3. SEM images of the indicated parts of the actuating hydrogels. A: D1G2.5GO2. B: Junction area of I and II (D1G2.5GO2 + N1S2GO2). C: N1S2GO2, D: Junction area of II and III (N1S2GO2 + D3G3CD8). E: D3G3CD8.

min after each actuation circle to compensate the water loss during the NIR irradiation.

Mechanical Test. Tensile strength of the hydrogels in rod shape was detected with a Shimadzu AG-X plus testing system under crosshead speed of 100 mm/min at room temperature. The strain was taken as the length change relative to the original length, and the stress was estimated on the cross section of the original sample. Silicon oil was coated on the sample surface to prevent water evaporation.

Shear creep of the D1G2.5GO2 hydrogel was monitored under a constant shear stress of 50 Pa with a stress controlled rheometer AR-G2 (TA) using a parallel plate fixture of diameter of 60 mm at four temperatures. Sandpaper (3 M 734 P240) was fixed on each plate surfaces to avoid slip of the sample during measurements. Temperature was controlled by a Peltier plate. Silicone oil was laid on the edge of the fixture to prevent water evaporation.

Scanning Electron Microscope Observation. Internal morphology of every parts of the hydrogels and junction area of the hydrogels was observed with a scanning electron microscope (SEM, Zeiss EVO 18) operated at 10.0 kV. The hydrogel was quickly frozen in liquid nitrogen and then freezing-dried for 3 days. Before observation, the freeze-dried gel was carefully sliced and sputtered with gold.

RESULTS AND DISCUSSION

Mechanical Properties. High mechanical performance is essential for the actuating hydrogel materials to ensure the efficient action as response to the external stimuli, especially for the present actuator composed of three different hydrogels. The integrity and mechanical strength of hydrogel actuators are essential for the actuating process. Figure 2 shows photos of the hydrogel actuator (D1G2.5GO2 + N1S2GO2 + D3G3CD8) in different states. The original sample with three trunks is uniform (Figure 2A). The color of Part II (N1S2GO2) becomes white when the it is irradiated by NIR due to the phase separation of the PNIPAAm gel (Figure 2B).[7] Other parts of the hydrogel display no obvious color change under NIR irradiation. It is worth noting that the junction area of different hydrogels is not identifiable, because the slight copolymerization probably occurred during preparation as there exited monomer mixture within this area. The copolymerization would enhance the connection of different hydrogels. The perfect connection of three hydrogel parts is also manifested through stretch of the entire hydrogel sample (Figures 2C, 2D, and 2E), where the sample is stretched to 300% without any rupture at the junction area. Furthermore, the stretched sample under NIR irradiation in Figures 2F and 2G also exhibits a similar color change.

We also observed the internal microstructure of the actuating hydrogels in dried state through SEM Figures 3A, 3C, and 3E present the three parts of I, II, and III, respectively. The pore size of parts I (D1G2.5GO2) and III (D3G3CD8) based on the

DOI: 10.1021/acsami.5b08248
ACS Appl. Mater. Interfaces 2015, 7, 23423−23430

PDMAA hydrogel is larger than that of part II (N1S2GO2) based on the PNIPAAm hydrogel, which may be attributed to the different affinities of polymer chains to water, affecting the sublimation rate during freeze-drying. For the junction area, both large and small porous size structures are observed from Figures 3B and 3D, revealing that the junction area is composed of the neighboring parts of hydrogels. The above results indicate that the three trunks of the hydrogels are combined tightly during the preparation.

Tensile behavior of every trunks of the actuating hydrogel was evaluated and Figure 4 depicts the stress−strain curves of

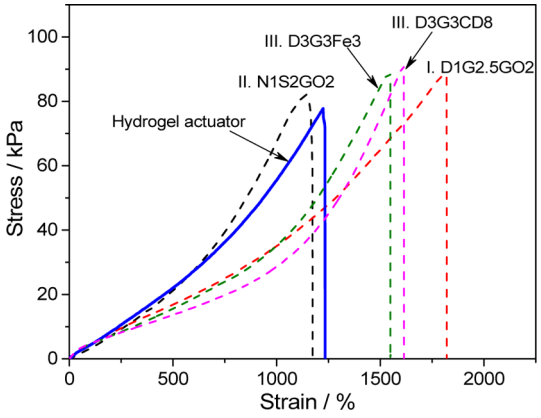

Figure 4. Tensile stress−strain curves of the actuating hydrogel (solid line) and its individual parts I (D1G2.5GO2), II (N1S2GO2), and III (D3G3CD8 and D1G3Fe3) (dashed lines).

an actuating hydrogel containing three trunks and the individual parts I−III. The tensile strength of these component hydrogels is 80−90 kPa, almost independent of the hydrogel composition studied. On the other hand, the elongation at break varies from 1200% to 1800%, depending on the hydrogel composition. Generally, PDMAA-clay hydrogels have maximum elongation larger than 1500%,[18,29] and the hydrogels containing less clay and monomer (D1G2.5GO2) shows a high elongation due to its lower cross-linking density. While the PNIPAAm-clay hydrogels are capable to be stretched up to about 1000%,[5,6,30] which is the case of the N1S2GO2 hydrogel in Figure 4.

For the entire actuating hydrogel, the tensile strength and elongation at break are about 78 kPa and 1220%, respectively, comparable with the weakest trunk (N1S2GO2) in these three component hydrogels. Actually, the fracture occurred at the N1S2GO2 hydrogel trunk, not at the junction areas. During preparation, the reaction solutions of three hydrogel parts were successively injected into one glass tube before polymerization. The stretch results combining with the above morphology indicate that this method succeeds in connecting three trunks of hydrogels together strongly. Because high viscosity of the reaction solutions limits the mutual diffusion across the interface, the feature of each trunk is maintained. At the same time, small amount of monomers are mixed in the junction area to be copolymerized to produce a strong joint for different hydrogel trunks.[28] Thus, the present hydrogel actuator has high mechanical strength without breakage at the junction areas.

Actuating Process. On the basis of the tough hybrid actuating hydrogel composed with three response trunks, we examined its actuating process under NIR irradiation. As schematically demonstrated in Figure 1B, part I extends under NIR irradiation, which allows part III, the "hand" or hook, to reach and catch the object by adhesion (Figure 1B 1 → 2). The adhesive hydrogel is realized by introducing α-CD into the PDMAA-clay hydrogel, where large amount of hydroxyl groups in α-CD molecules enhance the interaction between the hook and object through hydrogen bonding. (Detailed adhesive test of the adhesive hydrogel is provided by Figure S1.) Then, part II is irradiated with NIR, and the object is lifted during contraction of part II (Figure 1B 2 → 3).

The hook (part III) of the hybrid hydrogel actuator can be exchanged with a magnetic hydrogel by adding Fe_3O_4 nanoparticles in the polymerization suspension. This hook hydrogel is magnetically guided toward desired positions, more than just below the actuator (Figure 1C). The magnetically guiding actuation of the magnetic hydrogel is presented in Figure S2.

Figure 5A illustrates a conceptual example of the hybrid hydrogel actuator serving as an electrical circuit switch driven

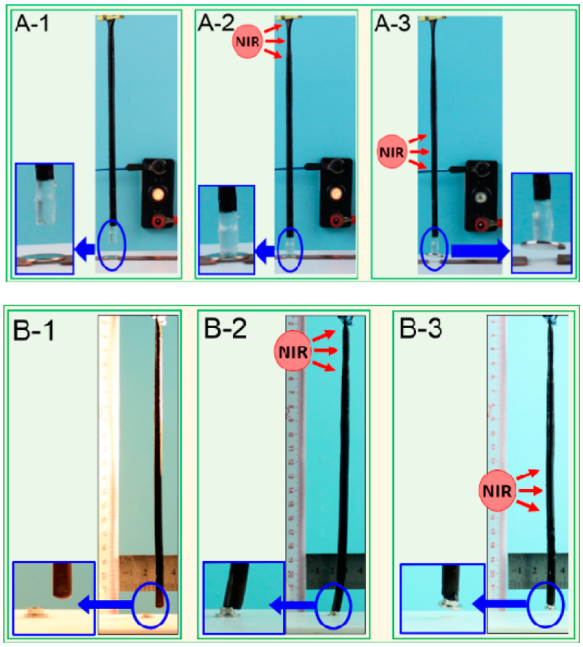

Figure 5. A: Photos of removing the sheet-metal switch (1.2 g) by the hybrid hydrogel actuator (A-1) driven by NIR irradiation successively on part I for extension and adhesion (A-2) and on part II for lifting (A-3). B: Photos of approach of the hybrid hydrogel actuator with magnetic hook (B-1) driven by NIR irradiation on part I and a magnet (B-2) on part III, and lifting weight (0.6 g) by irradiation on part II (B-3).

by NIR irradiation (complete electrical circuit in Figure S3). The hydrogel actuator extends and reaches the sheet-metal switch when irradiated on part I. The metal switch is captured by part III through adhesion. Then, the switch is raised by the contraction of part II under NIR irradiation, resulting in the lamp being switched-off. Figure 5B manifests the hybrid hydrogel actuator with the magnetic hook driven by both NIR irradiation and magnetic force. The actuator is horizontally shifted for about 10 mm driven by a magnet in addition to the extension and retraction in vertical direction driven by NIR irradiation. This actuator can be applied to collect magnetic particles in severe environments by remote control.

In the above case, the object is held with the hydrogel hook made of D3G3CD8. How to release the captured object from

DOI: 10.1021/acsami.5b08248
ACS Appl. Mater. Interfaces 2015, 7, 23423−23430

the hook? Here, we have designed an adhesion-tunable hook based on the hybrid hydrogel of N1S2GO2CD8 (Figure 6).

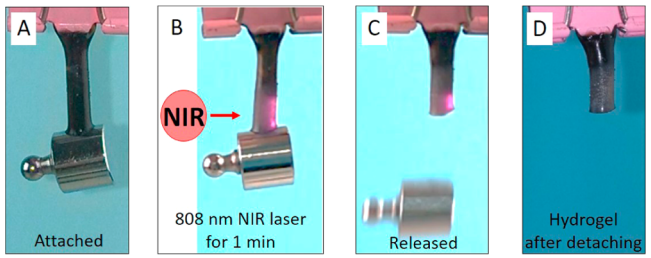

Figure 6. Release of captured object from the adhesive hydrogel N1S2GO2CD8 by irradiation of the 808 nm NIR laser. A: Attached state. B: Irradiating with a NIR laser on the adhesive interface. C: Release of the attached object. D: Hydrogel after detaching.

GO in the hydrogel transforms the NIR energy to thermal energy rapidly and efficiently to cause phase separation and dehydration of the PNIPAAm hydrogel. Then, the adhesive force is reduced and the captured object is released in 1 min.[31] The same idea is easily generalized by changing the hook (part III) for other purpose, for example, porous absorbents for water−oil separation or dye absorption and catalyst-loaded hydrogel for position-controlled reaction.[32]

To evaluate the actuating action quantitatively, we determined the length change of the hybrid actuating hydrogel under NIR irradiation. Figure 7 shows this length change ΔL related to the original length L_0 during the whole actuation process. During the first 10 s of irradiation on part I, there is no visible length change for preheating. Then, the hydrogel actuator begins to extend rapidly under the irradiation. When NIR is turned-off after irradiation for 30 s, the actuator extends continuously for about 60 s, and then stops at $\Delta L/L_0 \approx 11\%$. At this moment, Part III of the hydrogel actuator catches the object through adhesion or magnetic force. Part II of the hydrogel actuator is then irradiated with NIR, which contracts immediately, lifting the object. This contraction stops as soon as the NIR is turned-off, where $\Delta L/L_0 \approx 5\%$. The residual extension originates from the creep of part I and cannot be recovered by contraction of part II. The actual value of $\Delta L/L_0$ can be adjusted by the length of each part of the hydrogel actuator and the irradiation time, and the response rate of the hydrogel actuator can be regulated by tuning the cross-linking density and morphology of the hydrogels during polymerization.[33] The present actuator is conceptually designed to transform NIR energy to thermal energy and then to mechanical energy. Its energy transforming efficiency is still low (lower than 10^{-4}%) probably because of the unsatisfactory materials and multiple energy transformations. Therefore, great efforts to develop new hydrogels with high energy transforming efficiency are expected for the soft actuators.

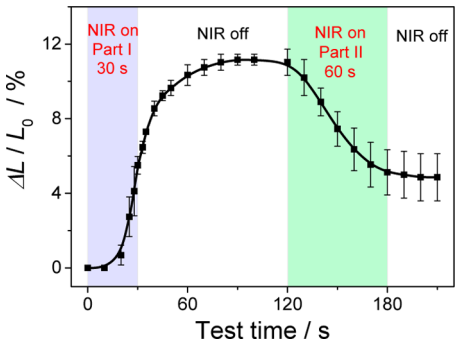

Figure 7. Relative length change of the hydrogel actuator during whole actuation with NIR irradiation on and off at parts I and II for the indicated time intervals of 30 and 60 s.

Actuation Mechanism. We explore the actuation mechanism of the hydrogel actuator with temperature response and creep behavior as illustrated in Figure 8. Figure 8A displays the temperature change of the component parts of the hydrogel actuator under NIR irradiation. The temperature increment of the hydrogels D1G2.5GO2 (part I) and N1S2GO2 (part II) containing GO is much faster (solid lines) than that of the corresponding hydrogels without GO (dashed lines). This is due to GO in the hydrogels, which absorbs the NIR energy and transforms it into thermal energy rapidly and efficiently.[11,14,24] As the temperature of the hydrogel N1S2GO2 reaches the volume phase transition temperature (VPTT, ~32 °C) of the PNIPAAm hydrogel[6,34] very quickly, part II begins to contract immediately without delay when NIR is on as shown in Figure 7.

We previously found that the PDMAA-clay hydrogel exhibited a thermal moldable behavior and large thermo-creep because of the thermo-reversible cross-linking.[35] Figure 8B depicts the shear creep strain of the hydrogel D1G2.5GO2 at four temperatures. The creep is small at 20 and 40 °C, but becomes large at 60 and 80 °C. Therefore, the hydrogel

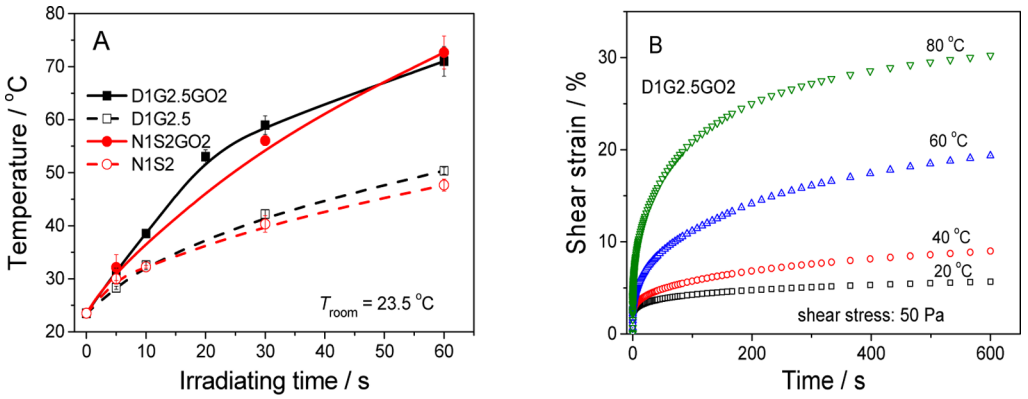

Figure 8. A: Temperature of indicated hydrogels as a function of NIR irradiation time. B: Shear strain creep of the hydrogel D1G2.5GO2 under stress of 50 Pa at indicated temperatures.

DOI: 10.1021/acsami.5b08248
ACS Appl. Mater. Interfaces 2015, 7, 23423−23430

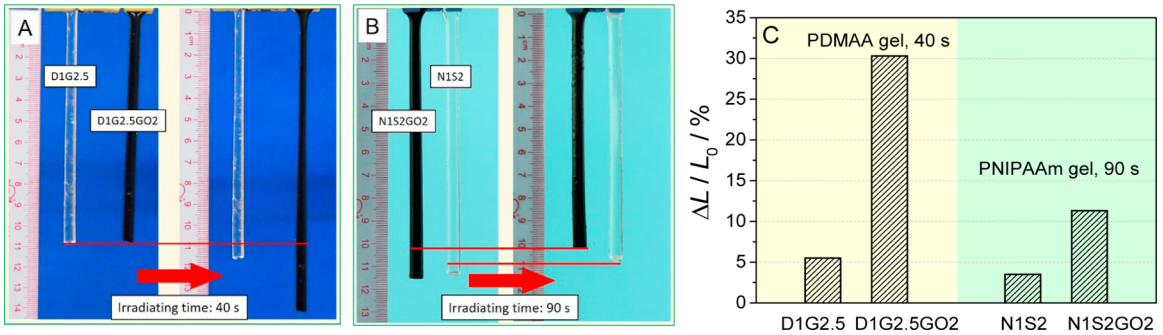

Figure 9. A: Length of PDMAA hydrogels D1G2.5 and D1G2.5GO2 before and after NIR irradiation. B: Length of PNIPAAm hydrogels N1S2GO2 and N1S2 before and after NIR irradiation. C: Relative length change $\Delta L/L_0$ of the hybrid hydrogels with and without GO under NIR irradiation for indicated time.

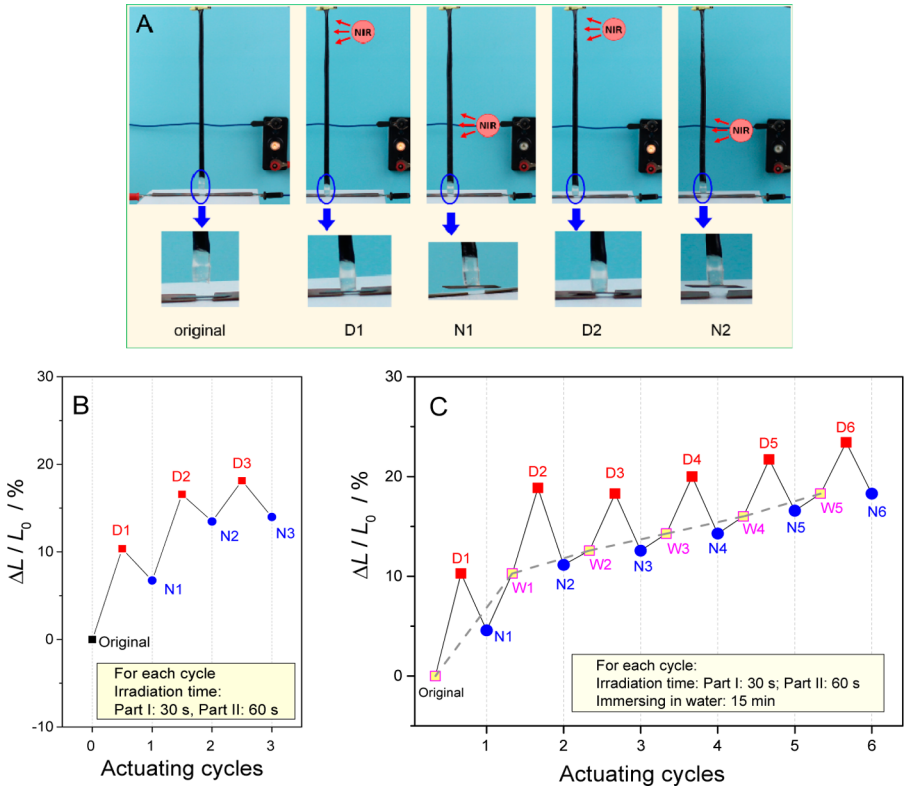

Figure 10. A: Two actuation cycles of the hybrid hydrogel actuator to operate an electrical circuit switch by successive irradiation on parts I and II. B: Relative length change of the hybrid hydrogel actuator upon repeat NIR irradiation with D*i* and N*i* denoting the *i*th irradiation on parts I and II, respectively. C: Relative length change of the hybrid hydrogel actuator during repeat NIR irradiation and water-immersing for 15 min (W*i*) after each cycle. The irradiation time on parts I and II is 30 and 60 s, respectively.

D1G2.5GO2 of part I extends upon thermo-creep under NIR irradiation. The 10 s preheating in Figure 7 for the hydrogel actuator at the beginning of irradiation is required to increase the temperature of part I to produce a detectable creep.

For visual and direct comparison, Figure 9 demonstrates the length change of the PDMAA-clay and PNIPAAm-clay hybrid hydrogels with and without GO under NIR irradiation. Passing the same irradiation time, the length of the PDMAA hydrogel containing GO is much longer than that of the corresponding hydrogel without GO (Figure 9A). On the other hand, when the same irradiation is carried out on the PNIPAAm hydrogel, lager contraction is achieved with GO in the hydrogel (Figure 9B). Addition of GO in the hydrogels greatly accelerates the temperature increment and promotes the actuation to be realized within 30 s. Upon the NIR irradiating, $\Delta L/L_0$ of D1G2.5GO2 reaches 30% within 40 s, while it is only about 12% for N1S2GO2 after 90 s irradiation (Figure 9C). Thus, the length change rate (slope of the curve in Figure 7) is fast for part I (after delay) and slow for part II.

The actuating accuracy of the hybrid hydrogel actuator can be improved by regulating the irradiation area on the hydrogels, in turn to control the length change of the hydrogel. This is tested by using a NIR laser, which exposes a finite area for 90 s and moves along the actuating hydrogel stepwise on part I (Figure S4). The extension of the hydrogel actuator, thus, is adjusted accurately.

The repeatability of actuating actions is desired for the soft actuators. Figure 10A presents two actuating cycles to manipulate an electrical circuit switch with the hybrid hydrogel actuator without any treatment. The actuating action is

DOI: 10.1021/acsami.5b08248
ACS Appl. Mater. Interfaces 2015, 7, 23423−23430

repeated just through the NIR irradiation on parts I and II alternately. The relative length change is plotted in Figure 10B as a function of the actuation cycle with D*i* and N*i* denoting the *i*th irradiation on parts I and II, respectively. Because of the water loss from the hydrogel during NIR irradiation, the actuation amplitude decreases with increasing cycle number.

To compensate the water loss, the actuating hydrogel was immersed in deionized water for 15 min after every actuation cycle. The relative weight change of an actuating hydrogel after actuation cycle and water-immersing treatment is shown in Figure S5. The weight change after each actuation cycle is about 10% caused by losing water, and the water-immersing treatment compensates the water loss almost completely. Figure 10C depicts the relative length change of the hybrid hydrogel actuator during six actuation circles, where the actuation amplitude is recovered and the entire length of the hydrogel increases gradually with increasing actuation cycles (dashed line). The length increase is induced by the thermo-creep of Part I under NIR irradiation as seen from Figures 7 and 8B, which cannot be recovered during actuation cycle and water-immersing. However, this residual extension of the hydrogel actuator is less than 20% of its original length in the present work.

CONCLUSIONS

In the present work, we were inspired by fishing rods and human arms and designed a hybrid hydrogel actuator consisting of series combination of three trunks of polymer−clay hydrogels with excellent mechanical strength and extensibility. The hydrogel trunks with thermo-creep and thermo-contraction functions were separately driven by NIR irradiation to execute extension and lifting actions, and the adhesive or magnetic hydrogel trunk acted as a hook to catch object. Therefore, this hybrid hydrogel actuator accomplished an extension−grasp−retraction comprehensive actuation, like a fishing rod. The GO in the hydrogels absorbed NIR energy and transformed it into thermal energy rapidly and effectively. The hook of the hybrid hydrogel actuator was replaceable according to applications, even with functional materials other than hydrogels. Based on this design, the driving source can be programed with a mask to guide the irradiating position and area on the hydrogels with gradient composition and/or bilayer structure. Bioinspired versatile hydrogel actuators can be developed in this way.

ASSOCIATED CONTENT

Supporting Information

The Supporting Information is available free of charge on the ACS Publications website at DOI: 10.1021/acsami.5b08248.

Preparation of Fe_3O_4 magnetic nanoparticles, adhesive and magnetic properties tests, electric circuit, and accurate actuation under NIR laser irradiation, as well as the relative weight change during the repeat actuations (PDF)

AUTHOR INFORMATION

Corresponding Author

*E-mail: mcztong@scut.edu.cn. Tel: (86)-20-87112886. Fax: (86)-20-87110273.

Notes

The authors declare no competing financial interest.

ACKNOWLEDGMENTS

The financial support from the NSFC (21427805 and 51203052), the National Basic Research Program of China (973 Program, 2012CB821504), the Fundamental Research Funds for the Central Universities (2015ZM051 and 2015ZP005), and the Excellent Doctoral Dissertation Project of Guangdong Province of China (SYBZZXM201312) are gratefully acknowledged.

REFERENCES

(1) Okuzaki, H. *Soft Actuators*, 1st ed.; Springer: Tokyo, 2014.
(2) Lim, H. L.; Hwang, Y.; Kar, M.; Varghese, S. Smart Hydrogels as Functional Biomimetic Systems. *Biomater. Sci.* **2014**, *2*, 603−618.
(3) Doering, A.; Birnbaum, W.; Kuckling, D. Responsive Hydrogels - Structurally and Dimensionally Optimized Smart Frameworks for Applications in Catalysis, Micro-system Technology and Material Science. *Chem. Soc. Rev.* **2013**, *42*, 7391−7420.
(4) Naficy, S.; Brown, H. R.; Razal, J. M.; Spinks, G. M.; Whitten, P. G. Progress Toward Robust Polymer Hydrogels. *Aust. J. Chem.* **2011**, *64*, 1007−1025.
(5) Haraguchi, K.; Takehisa, T. Nanocomposite Hydrogels: a Unique Organic-Inorganic Network Structure with Extraordinary Mechanical, Optical, and Swelling/De-swelling Properties. *Adv. Mater.* **2002**, *14*, 1120−1124.
(6) Zhang, E.; Wang, T.; Lian, C.; Sun, W.; Liu, X.; Tong, Z. Robust and Thermo-response Graphene−PNIPAm Hybrid Hydrogels Reinforced by Hectorite Clay. *Carbon* **2013**, *62*, 117−126.
(7) Zhang, E.; Wang, T.; Hong, W.; Sun, W.; Liu, X.; Tong, Z. Infrared-Driving Actuation Based on Bilayer Graphene Oxide-Poly(*N*-isopropylacrylamide) Nanocomposite Hydrogels. *J. Mater. Chem. A* **2014**, *2*, 15633−15639.
(8) Sun, J. Y.; Zhao, X.; Illeperuma, W. R. K.; Chaudhuri, O.; Oh, K. H.; Mooney, D. J.; Vlassak, J. J.; Suo, Z. Highly Stretchable and Tough Hydrogels. *Nature* **2012**, *489*, 133−136.
(9) Sun, T. L.; Kurokawa, T.; Kuroda, S.; Ihsan, A. B.; Akasaki, T.; Sato, K.; Haque, M. A.; Nakajima, T.; Gong, J. P. Physical Hydrogels Composed of Polyampholytes Demonstrate High Toughness and Viscoelasticity. *Nat. Mater.* **2013**, *12*, 932−937.
(10) Bin Imran, A.; Esaki, K.; Gotoh, H.; Seki, T.; Ito, K.; Sakai, Y.; Takeoka, Y. Extremely Stretchable Thermosensitive Hydrogels by Introducing Slide-ring Polyrotaxane Cross-linkers and Ionic Groups into the Polymer Network. *Nat. Commun.* **2014**, *5*, 5124.
(11) Acik, M.; Lee, G.; Mattevi, C.; Chhowalla, M.; Cho, K.; Chabal, Y. J. Unusual Infrared-Absorption Mechanism in Thermally Reduced Graphene Oxide. *Nat. Mater.* **2010**, *9*, 840−845.
(12) Robinson, J. T.; Tabakman, S. M.; Liang, Y.; Wang, H.; Sanchez Casalongue, H.; Vinh, D.; Dai, H. Ultrasmall Reduced Graphene Oxide with High Near-Infrared Absorbance for Photothermal Therapy. *J. Am. Chem. Soc.* **2011**, *133*, 6825−6831.
(13) Feng, L.; Wu, L.; Qu, X. New Horizons for Diagnostics and Therapeutic Applications of Graphene and Graphene Oxide. *Adv. Mater.* **2013**, *25*, 168−186.
(14) Li, W.; Wang, J.; Ren, J.; Qu, X. 3D Graphene Oxide−Polymer Hydrogel: Near-Infrared Light-Triggered Active Scaffold for Reversible Cell Capture and On-Demand Release. *Adv. Mater.* **2013**, *25*, 6737−6743.
(15) Huang, W.; Shen, J.; Li, N.; Ye, M. Study on a New Polymer/Graphene Oxide/Clay Double Network Hydrogel with Improved Response Rate and Mechanical Properties. *Polym. Eng. Sci.* **2015**, *55*, 1361−1366.
(16) Cong, H.-P.; Wang, P.; Yu, S.-H. Stretchable and Self-Healing Graphene Oxide-Polymer Composite Hydrogels: A Dual-Network Design. *Chem. Mater.* **2013**, *25*, 3357−3362.
(17) Auletta, J. T.; LeDonne, G. J.; Gronborg, K. C.; Ladd, C. D.; Liu, H.; Clark, W. W.; Meyer, T. Y. Stimuli-Responsive Iron-Cross-Linked Hydrogels That Undergo Redox-Driven Switching between Hard and Soft States. *Macromolecules* **2015**, *48*, 1736−1747.

DOI: 10.1021/acsami.5b08248
ACS Appl. Mater. Interfaces 2015, 7, 23423−23430

(18) Zhang, E.; Wang, T.; Zhao, L.; Sun, W.; Liu, X.; Tong, Z. Fast Self-Healing of Graphene Oxide-Hectorite Clay-Poly(*N,N*-dimethylacrylamide) Hybrid Hydrogels Realized by Near-Infrared Irradiation. *ACS Appl. Mater. Interfaces* **2014**, *6*, 22855−22861.
(19) Du, G.; Nie, L.; Gao, G.; Sun, Y.; Hou, R.; Zhang, H.; Chen, T.; Fu, J. Tough and Biocompatible Hydrogels Based on in Situ Interpenetrating Networks of Dithiol-Connected Graphene Oxide and Poly(vinyl alcohol). *ACS Appl. Mater. Interfaces* **2015**, *7*, 3003−3008.
(20) Yu, Y.; De Andrade, L.; Fang, L.; Ma, J.; Zhang, W.; Tang, Y. Graphene Oxide and Hyperbranched Polymer-Toughened Hydrogels with Improved Absorption Properties and Durability. *J. Mater. Sci.* **2015**, *50*, 3457−3466.
(21) Won, D.-A.; Kim, M.; Tae, G. Systemic Modulation of the Stability of Pluronic Hydrogel by a Small Amount of Graphene Oxide. *Colloids Surf., B* **2015**, *128*, 515−521.
(22) Shen, J.; Xin, X.; Zhang, Y.; Song, L.; Wang, L.; Tang, W.; Ren, Y. Manipulation the Behavior of Supramolecular Hydrogels of α-Cyclodextrin/Star-like Block Copolymer/Carbon-based Nanomaterials. *Carbohydr. Polym.* **2015**, *117*, 592−599.
(23) Cong, H.-P.; Qiu, J.-H.; Yu, S.-H. Thermoresponsive Poly(*N*-isopropylacrylamide)/ Graphene/Au Nanocomposite Hydrogel for Water Treatment by a Laser-Assisted Approach. *Small* **2015**, *11*, 1165−1170.
(24) Liang, J.; Xu, Y.; Huang, Y.; Zhang, L.; Wang, Y.; Ma, Y.; Li, F.; Guo, T.; Chen, Y. Infrared-Triggered Actuators from Graphene-Based Nanocomposites. *J. Phys. Chem. C* **2009**, *113*, 9921−9927.
(25) Kim, S.; Laschi, C.; Trimmer, B. Soft Robotics: a Bioinspired Evolution in Robotics. *Trends Biotechnol.* **2013**, *31*, 23−30.
(26) Ilievski, F.; Mazzeo, A. D.; Shepherd, R. F.; Chen, X.; Whitesides, G. M. Soft Robotics for Chemists. *Angew. Chem., Int. Ed.* **2011**, *50*, 1890−1895.
(27) Hummers, W. S.; Offeman, R. E. Preparation of Graphitic Oxide. *J. Am. Chem. Soc.* **1958**, *80*, 1339−1339.
(28) Banik, S. J.; Fernandes, N. J.; Thomas, P. C.; Raghavan, S. R. A New Approach for Creating Polymer Hydrogels with Regions of Distinct Chemical, Mechanical, and Optical Properties. *Macromolecules* **2012**, *45*, 5712−5717.
(29) Haraguchi, K.; Farnworth, R.; Ohbayashi, A.; Takehisa, T. Compositional Effects on Mechanical Properties of Nanocomposite Hydrogels Composed of poly(N,N-dimethylacrylamide) and Clay. *Macromolecules* **2003**, *36*, 5732−5741.
(30) Wang, T.; Liu, D.; Lian, C.; Zheng, S.; Liu, X.; Tong, Z. Large Deformation Behavior and Effective Network Chain Density of Swollen Poly(*N*-isopropylacrylamide)-Laponite Nanocomposite Hydrogels. *Soft Matter* **2012**, *8*, 774−783.
(31) Wang, T.; Yang, Y.; Sun, W.; Wang, C.; Liu, X.; Tong, Z. Infrared Radiation Triggered Detachable Bio-adhesive Hybrid Hydrogels. *J. Controlled Release* **2015**, *213*, e102−e103.
(32) Ruan, C.; Ai, K.; Li, X.; Lu, L. A Superhydrophobic Sponge with Excellent Absorbency and Flame Retardancy. *Angew. Chem., Int. Ed.* **2014**, *53*, 5556−5560.
(33) Zheng, S.; Wang, T.; Liu, D.; Liu, X.; Wang, C.; Tong, Z. Fast Deswelling and Highly Extensible Poly(*N*-isopropylacrylamide)-Hectorite Clay Nanocomposite Cryogels Prepared by Freezing Polymerization. *Polymer* **2013**, *54*, 1846−1852.
(34) Hu, X.; Xiong, L.; Wang, T.; Lin, Z.; Liu, X.; Tong, Z. Synthesis and Dual Response of Ionic Nanocomposite Hydrogels with Ultrahigh Tensibility and Transparence. *Polymer* **2009**, *50*, 1933−1938.
(35) Yang, Y.; Wang, T.; Sun, W.; Wang, C.; Liu, X.; Tong, Z. Thermo-Moldable Nanocomposite Hydrogels. *Macromol. Mater. Eng.* **2015**, *300*, 57−63.

DOI: 10.1021/acsami.5b08248
ACS Appl. Mater. Interfaces 2015, 7, 23423−23430